Quaternary Science Reviews 125 (2015) 50–60

Contents lists available at ScienceDirect

Quaternary Science Reviews

journal homepage: www.elsevier.com/locate/quascirev

Research paper

Indian monsoon variations during three contrasting climatic periods: The Holocene, Heinrich Stadial 2 and the last interglacial–glacial transition

Coralie Zorzi [a, *], Maria Fernanda Sanchez Goñi [a], Krishnamurthy Anupama [b], Srinivasan Prasad [b], Vincent Hanquiez [c], Joel Johnson [d], Liviu Giosan [e]

[a] Ecole Pratique des Hautes Etudes, UMR CNRS 5805 EPOC, Université de Bordeaux, 33405 Talence, France
[b] Laboratory of Palynology & Paleoecology, French Institute of Pondicherry PB 33 UMIFRE 21 CNRS-MAEE/USR 3330, Pondicherry 605001, India
[c] Université de Bordeaux, UMR CNRS 5805 EPOC, 33405 Talence, France
[d] University of New Hampshire, Department of Earth Sciences, James Hall, Durham, NH 03824-3589, USA
[e] Geology & Geophysics, Woods Hole Oceanographic Institution, Woods Hole, MA 02543, USA

ARTICLE INFO

Article history:
Received 26 December 2014
Received in revised form
3 June 2015
Accepted 9 June 2015
Available online xxx

Keywords:
Indian summer monsoon
Core Monsoon Zone
Pollen assemblage
Holocene
Heinrich Stadial 2
Last interglacial–glacial transition

ABSTRACT

In contrast to the East Asian and African monsoons the Indian monsoon is still poorly documented throughout the last climatic cycle (last 135,000 years). Pollen analysis from two marine sediment cores (NGHP-01-16A and NGHP-01-19B) collected from the offshore Godavari and Mahanadi basins, both located in the Core Monsoon Zone (CMZ) reveals changes in Indian summer monsoon variability and intensity during three contrasting climatic periods: the Holocene, the Heinrich Stadial (HS) 2 and the Marine Isotopic Stage (MIS) 5/4 during the ice sheet growth transition. During the first part of the Holocene between 11,300 and 4200 cal years BP, characterized by high insolation (minimum precession, maximum obliquity), the maximum extension of the coastal forest and mangrove reflects high monsoon rainfall. This climatic regime contrasts with that of the second phase of the Holocene, from 4200 cal years BP to the present, marked by the development of drier vegetation in a context of low insolation (maximum precession, minimum obliquity). The historical period in India is characterized by an alternation of strong and weak monsoon centennial phases that may reflect the Medieval Climate Anomaly and the Little Ice Age, respectively. During the HS 2, a period of low insolation and extensive iceberg discharge in the North Atlantic Ocean, vegetation was dominated by grassland and dry flora indicating pronounced aridity as the result of a weak Indian summer monsoon. The MIS 5/4 glaciation, also associated with low insolation but moderate freshwater fluxes, was characterized by a weaker reduction of the Indian summer monsoon and a decrease of seasonal contrast as recorded by the expansion of dry vegetation and the development of *Artemisia*, respectively. Our results support model predictions suggesting that insolation changes control the long term trend of the Indian monsoon precipitation, but its millennial scale variability and intensity are instead modulated by atmospheric teleconnections to remote phenomena in the North Atlantic, Eurasia or the Indian Ocean.

1. Introduction

The Indian monsoon brings more than 80% of the annual rainfall to the Central Indian peninsula (Gadgil, 2003). Identifying its natural rhythmicity, magnitude, and the physical processes involved is a challenge for present-day and future socio-economic policy predictions. Model studies (Broccoli et al., 2006; Chiang et Bits, 2005; Mohtadi et al., 2014; Pausata et al., 2011; Vernekar et al., 1995) and palaeoclimatic observations (Agnihotri et al., 2002; Fleitmann et al., 2007; Gupta et al., 2003; Hahn et al., 1976; Ponton et al., 2012; Sinha et al., 2007) suggest that abrupt changes of Indian monsoon are in phase with North Atlantic climate variations. These studies further show that changes in the Intertropical Convergence Zone (ITCZ), North Atlantic iceberg discharges, Indian Ocean sea surface temperature (SST) gradient and Himalayan snow cover can explain the rapid atmospheric

* Corresponding author.
E-mail address: coraliezorzi@gmail.com (C. Zorzi).

http://dx.doi.org/10.1016/j.quascirev.2015.06.009
0277-3791/

reorganization between the North Atlantic and the Indian region. However, few high temporal resolution studies have been done on the main region preferentially affected at present by the summer monsoon, i.e. the Core Monsoon Zone (CMZ), and under different climate regimes (e.g. Ponton et al., 2012 for the Holocene Godavari basin and Prasad et al., 2014 for the crater lake Lonar in the Holocene).

To fill this gap we performed pollen analysis on two marine sediment cores collected in the slope environment in the western Bay of Bengal off the Godavari and Mahanadi rivers and focused on three contrasting climatic periods of the last climatic cycle, i.e. the Holocene, Heinrich Stadial (HS) 2 (~26,000–24,000 years cal BP), and the last interglacial–glacial transition (~73,000 years ago). These cores are ideally suited to reconstruct Indian summer monsoon variability because they preserved pollen assemblages from the regional vegetation occupying the Godavari and Mahanadi hydrographic basins that are both located in the CMZ (Fig. 1). Pollen assemblages preserved in marine sediments located close to river mouths accurately represent an integrated image of the regional vegetation, and therefore climate, in the related hydrological basins (e.g. Dupont and Wyputta, 2003; Heusser, 1985; Naughton et al., 2007). Consequently, the pollen assemblages from the eastern part of the Indian margin are a powerful tool to reconstruct monsoon variability in the CMZ.

2. Present-day environmental setting

2.1. Climate: oceanographic and atmospheric processes

The present-day climate of the Indian peninsula is controlled by the monsoon (Attri and Tyagi, 2010; Walter, 1961). The strong insolation during summer (June–September) leads to a strong atmospheric pressure gradient between the Indian Ocean and India that generates the humid and warm winds of the Indian summer monsoon (Fig. 1). During winter months (December–February), the pressure gradient reverses due to weak insolation and the dry and cold winds of the Indian winter monsoon cross over India from the East Asian continent to the Arabian Sea (Fig. 1).

The magnitude of the Indian summer monsoon is the result of the dynamics of three spatial components associated respectively to three heating gradients (Caley, 2011; Webster et al., 1998): a) North-South gradient (lateral monsoon) that is associated with the insolation-derived ITCZ migrations, b) East-West component (transversal monsoon) driven by longitudinal heating gradients linked to SST oscillations of the Indian Ocean Dipole, and c) an altitudinal component depending on Walker circulation (Caley, 2011). Lateral and transversal monsoonal variations during the boreal summer are the main components affecting monsoon variations (Webster et al., 1998). Both orbitally-controlled ITCZ seasonal migrations and continental influences from the northern regions determine rainfall distribution across the Indian sub-continent. Indian Dipole oscillations impact, in turn, the amount of humidity brought by the oceanic winds during the summer monsoon period; the southern part of the Indian Ocean is the major source of moisture to the Indo-Asian monsoon systems (Yihui et al., 2004). The Tibetan plateau also has an important thermodynamic and atmospheric impact, especially on the seasonal temperature contrast through the albedo feedback, and therefore on the monsoon intensity (Araya-Melo et al., 2014; Gunnell et al., 1997; Ruddiman and Kutzbach, 1991).

2.2. The Core Monsoon Zone and its vegetation

The Indian summer monsoon rainfall starts in the western coastal range of the Western Ghats and progressively reaches the rest of the peninsula with rainfall decreasing along a SW–NE negative gradient. In the Central and North-Eastern part of India, a second branch of the monsoon follows the Bay of Bengal Coast from the south to the north and contributes to the total summer rainfall in these areas. The CMZ is defined as the area in which the variation of rainfall during the months of July and August represents well the intensity of the annual Indian summer monsoon (Fig. 1). This zone, very sensitive to Indian summer variations, is therefore a key region for the identification of weak or intense monsoon periods, referred to break and active spells, respectively (Rajeevanand Gadgil, 2008).

In India, the natural vegetation distribution depends on three factors: annual average rainfall, length of the dry season, and mean temperature of the coldest month (Gaussen et al., 1965; Gunnell, 1997). In mountainous regions, vegetation distribution is also determined by temperature variations following the altitudinal gradient. However, below 900 m, the amount and seasonal distribution of annual rainfall are the most important factors on the vegetation distribution (Bonnefille et al., 1999). Most of the Godavari and Mahanadi river catchments are located in the CMZ and below 900 m (excluding the highest summits of the Eastern Ghats), and hence the vegetation responds to monsoon influence directly. Therefore, pollen-derived vegetation records from these areas will reflect variations in monsoon frequency and magnitude.

At present, CMZ vegetation is characterized by two main vegetation communities (biomes) according to the seasonal monsoon gradient (Fig. 1): *Thorny Vegetation* and *Tropical Deciduous Forest*. Within the *Tropical Deciduous Forest* two distinct forest types occur: the *Tropical Moist Deciduous Forest* (*TMDF*) and the *Tropical Dry Deciduous Forest* (*TMDF*) (Legris, 1963; Gaussen et al., 1965). Near the mouths of the Godavari and Mahanadi rivers, coastal communities such as mangroves, marshland and Arecaceae crops develop in association with these biomes (Fig. 2). The ecological requirements of these different plants are presented in Table 1. In the fossil record, mangroves, mainly characterized by Rhizophoraceae represent humid and saline coastal vegetation; its biodiversity, growth and development influenced by both marine dynamics (i.e., sea level variation, flooding and salinity) and fluvial input (i.e., fresh water and nutrients) (Hait and Behling, 2009). Marshlands composed of herbs and halophyte species, such as *Suaeda* sp. (Amaranthaceae), occupy hyper-saline areas of coastal regions. Arecaceae species, *Cocos* and *Borassus* trees, mostly considered as cultivated trees, can grow on salty and rich organic soils near mangrove areas. *Borassus flabellifer* presents a large range of rainfall tolerance, from 500 to 5000 mm average annual rainfall. Its constant association with *Cocos nucifera* that develops preferentially when the average annual rainfall is between 1000 and 1500 mm, indicates that these trees both belong to the coastal forest biome. High proportions of this forest in the past therefore represent periods of warm and moist conditions (Johnson, 2010). Poaceae, Cyperaceae and Amaranthaceae constitute the herbaceous vegetation that characterizes open environments. Nevertheless, Poaceae prefers dry areas (Bonnefille et al., 1999) and Cyperaceae moist conditions (Kraus et al., 2003). *Suaeda* sp. (Amaranthaceae) colonizes hypersaline zones close to mangrove vegetation (Hait and Behling, 2009). The pollen of this genus cannot be distinguished from that of the other genus included in the Amaranthaceae pollen morphotype, but considering the Godavari coastal ecological context (Selvam, 2003) we assume that the record of Amaranthaceae pollen percentages results from variations in the amount of *Suaeda* sp. in the Godavari and Mahanadi basins.

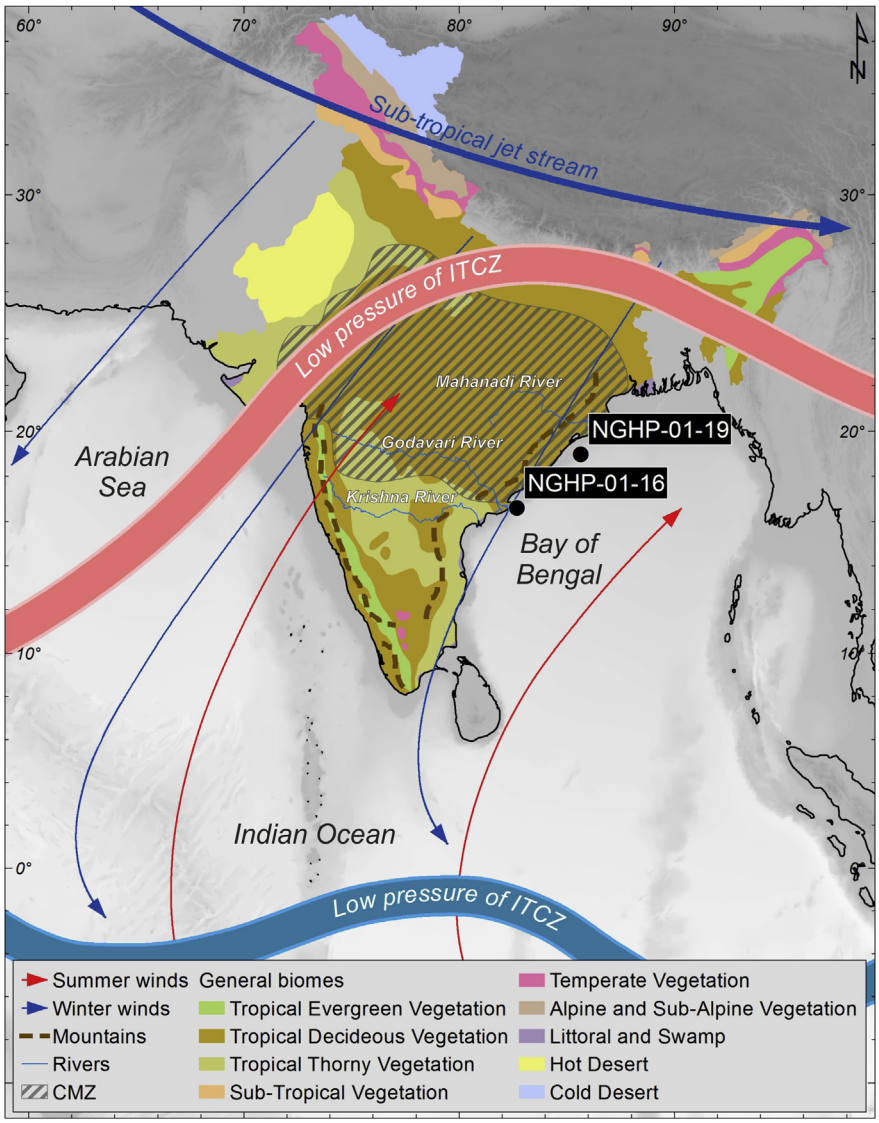

Fig. 1. The Core Monsoon Zone and the main Indian ecological zones associated with seasonal atmospheric variations showed by opposite ITCZ positions and monsoon wind directions. During the summer monsoon months ITZC is in northern position (pink line) and moist/warm winds (red arrows) cross India from the South-West to North-East. In winter ITCZ is in southern position (blue line) and dry/cold winds (blue arrows) cross India from North-East to South-West. General biomes from www.mapsofindia.com; ITCZ and wind location from www.geogonline.org.uk.

3. Materials and methods

3.1. Marine cores

We analyzed samples from marine sediment cores NGHP-01-16A and NGHP-01-19B collected on the western Bay of Bengal slope offshore the outlets of two of largest rivers of Central India during the first expedition (NGHP-01) of the Indian National Gas Hydrate Program (Collett et al., 2008). The portion of core NGHP-01-16A (16°35.59′N/082°41.00′E, 1265 m water depth, 217 m total length) sampled in this study (0–875 cm) covers the entire Holocene until HS 2. The sediments are composed of smectite-dominated hemipelagic clays commonly bearing calcareous nannofossils, foraminifera, and silt/sand lamina/beds (Phillips et al., 2014a) and terrestrial dominated organic carbon (Johnson et al., 2014) originating from the Godavari River during the last 27,000 years cal BP (Ponton et al., 2012). We also studied samples from core NGHP-01-19B (18°58.66′N/85°39.52′E, 1433 m water depth, 26 m total length) that was collected close to the Mahanadi River outlet. Core NGHP-01-19B is located north of site NGHP-01-16A and the base of this core records MIS 5d, capturing the last interglacial–glacial transition (MIS 5/4) (Phillips et al., 2014b). The illite-dominated hemipelagic clays in core NGHP-01-19B (Phillips et al., 2014a), contain calcareous nannofossils and foraminifera, and terrestrial dominated organic carbon (Johnson et al., 2014). The NGHP-01-19B core location is nearest to the Mahanadi River, but may also be influenced by the discharges of other CMZ rivers (Phillips et al., 2014a), thus the variations in the ecological assemblages observed in our study should reflect Indian monsoon variability and magnitude. Lithostratigraphic characteristics indicate that mass transfer events played no role in sedimentation at our sites for the periods considered in our study (Collet et al., 2008; Ponton et al., 2012; Phillips et al., 2014b).

The narrow continental shelf on the western side of the Bay of Bengal (Rao et al., 2012) reduces effects of sea level changes during

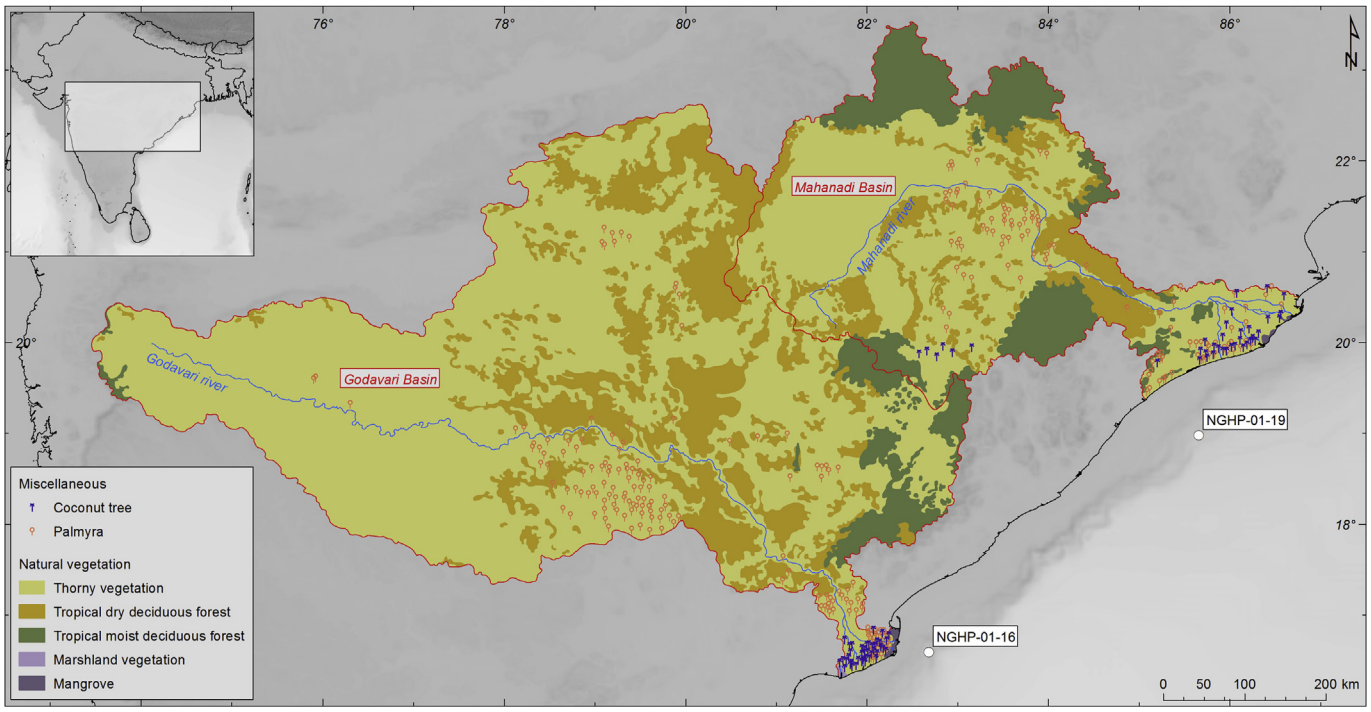

Fig. 2. Location of the studied sites and the distribution of the different ecological communities in the Godavari and Mahanadi basins. Ecological communities have been compiled from seven IFP maps published between 1963 and 1973 by Gaussen and colleagues.

the Holocene, the HS 2 and the MIS 5/4 transition. We do not expect therefore large variations in the distance between the Mahanadi and Godavari river mouths and the position of the coring sites. Thus, we consider that Mahanadi and Godavari catchments have remained practically identical through the time interval considered in our study.

3.2. Age model

The age model for core NGHP-01-16A was established by Ponton et al. (2012) using 11 ^{14}C dates. The measurements were performed on samples composed of mixed planktonic foraminifers >150 μm at the National Ocean Sciences Accelerator Mass Spectrometry Facility in Woods Hole (MA, USA) (see supplementary information/auxiliary material in Ponton et al., 2012). Using the CALIB 6.0 software (Stuiver and Reimer, 1993) and the Marine09 calibration curve (Reimer et al., 2009), the radiocarbon ages were converted to calendar ages. Available reservoir estimates for the Bay of Bengal surface waters are almost similar to the standard marine reservoir correction (Dutta et al., 2001; Southon et al., 2002; Ponton et al., 2012), which justify a surface water correction of 400 years. The age model was obtained by linear interpolation.

The age model for core NGHP-01-19B was established by Phillips et al. (2014b) using a combination of six radiocarbon dates between 0.01 and 6.188 m below sea floor (mbsf) and six oxygen isotopic events between 3.105 and 11.505 mbsf from the analysis of the benthic foraminifera *Uvigerina peregrina*. Radiocarbon ages were calibrated using the same protocol as applied for core NGHP-01-16A. The isotopic chronology follows the chronostratigraphy of Imbrie et al. (1984) and Martinson et al. (1987) and indicates that core NGHP-01-19B extends back to MIS 5d dated at around 111ka. The composition of an ash layer found at 8.42–8.46 m indicates that it originated from the Toba eruption, which is dated at approximately 71 ka. This age confirms the isotopic chronostratigraphy of core NGHP-01-19B.

3.3. Pollen analysis

The preparation technique for pollen analysis followed the protocol established at the UMR EPOC, University of Bordeaux (http://ephe-paleoclimat.com/ephe/Pollen%20sample%

Table 1
Natural biomes of the Godavari basin depending on the annual average rainfall and the length of the dry season along with the respective characteristic species after Gaussen et al., 1965; Pullaiah and Chennaian, 1997; Bonneffille et al., 1999; Selvam, 2003; Johnson, 2010.

Biome	Average annual rainfall (mm)	Length of dry season (months)	Characteristic plants
Tropical moist deciduous forest	1100–2000	4–7	*Mallotus* (Euphorbiaceae) *Olea glandulifera*(Oleaceae)
Tropical dry deciduous forest	500–1500	6–8	*Ixora* (Rubiaceae) *Manilkara* (Sapotaceae)
Thorny vegetation	<500	7–8	*Acacia* (Mimosaceae) *Dodonaea* (Sapindaceae)
Mangrove	>1500	No numerical data	Rhizophoraceae
Coastal forest	Moist conditions, no numerical data		*Borassus* (Arecaceae) *Cocos nucifera* (Arecaceae)
Marshland	Dry conditions, no numerical data		*Suaeda* sp. (Amaranthaceae)

20preparation.htm). After chemical treatment (cold HCl and cold HF) the samples were sieved through 10 μm nylon mesh screens. The final residue for pollen analysis was mounted unstained in bidistilled glycerine, which allows the mobility of the pollen grains to optimize their analysis. Identification and quantification of pollen grains were made at 400X and 1000X (oil immersion) magnifications using OLYMPUS CH20 and LEICA DFC295 microscopes at the French Institute of Pondicherry (or Institut Français de Pondicherry - IFP) and in the UMR EPOC, respectively. Pollen identification was based on the reference collection at IFP. Between 100 and 168 pollen grains and at least 20 pollen morphotypes were counted in each sample. The percentage of each pollen morphotype was calculated based on the main pollen sum that includes all the pollen grains excluding the spores of ferns. The ecological groups, or biomes, defined in this study are based on previous works and summarized in section 2.2 (Bonnefille et al., 1999; Gaussen et al., 1965; Hait and Belhing, 2009; Kraus et al., 2003; Legris, 1963; Selvam, 2003). In each sample, the percentages of different biomes are calculated as the sum of the percentages of the different morphotypes with the same ecological affinities. Pollen analysis was performed on 45 samples from the Holocene interval, 2 samples from the period chronologically assigned to the HS 2, and 13 samples from the MIS 5/4 transition. The temporal resolution is 150 years for the last 2000 years and 300 years for the rest of the Holocene. On average, the spatial resolution of the sampling was every 20 cm for the Holocene, 10 cm for the MIS 5/4 transition and the two samples from the HS 2 were spaced by 20 cm. The detailed pollen diagrams of the three climatic intervals were analyzed visually (Figures S1 and S2). In addition, we used *chclst* function from R package Rioja (Juggins, 2009) to perform a constrained hierarchical clustering analysis based on Euclidean distance between Holocene's samples (Figure S3). This analysis confirmed the pollen zones established by visual inspection. Lastly, we obtained an average pollen assemblage representing the moist period of the Holocene, the HS 2 and the MIS 5/4 transition by calculating the mean of the pollen percentages of the different ecological communities from 45, 2 and 13 samples, respectively. These average pollen assemblages are represented as pie charts.

We further performed a semi-quantitative comparison between present-day vegetation in Godavari basin based on the Godavari bio-climate map (Gaussen et al., 1965) and the pollen assemblage of the top-most sample of core NGHP-01-16A at 0–2 cm representing the last decades using ArcGIS software. This comparison between the present-day pollen assemblage and vegetation cover and composition allowed us to confirm that the pollen preserved in the marine cores used on our study off the outlets of Godavari and Mahanadi rivers accurately records the vegetation occupying their catchment areas and to better interpret our fossil pollen diagram in terms of vegetation and climate changes.

4. Results

4.1. Present day vegetation vs.the top-most pollen sample of core NGHP-01-16A

Mangrove and coastal assemblages are almost absent, and the *TMDF* is weakly represented in both the bio-climate map and the pollen assemblages of the top-most core sample (Table 2). In contrast, the marshland vegetation appears over represented in the marine pollen assemblage whilethorny and *TDDF* communities are better represented in the bio-climate map than in the top-most core sample. Two reasons can explain these two discrepancies:

a) Pollen assemblages in marine sediment cores preferentially record the ecological communities occupying coastal areas of a river catchment rather than pollen from regions located far inland in the catchment area. This hypothesis is supported by the good representation of the pollen record of coastal communities (mangrove and coastal forest) and the *TMDF* located on the Eastern part of Godavari catchment. It also explains the lower thorny vegetation pollen percentage found in the marine record, which represents the main community in the western part of the Godavari basin (Fig. 2).
b) The fact that we chose to distinguish in the pollen assemblage the cosmopolitan herbs Poaceae and Cyperaceae (grasslands) from main and classic dry vegetation, despite the observations that: a) herbaceous plants in the Godavari basin, including grasses, grow up preferentially on dry and open environments slightly affected by monsoon rainfalls (Gaussen et al., 1965) and b) in Central India, grasses have similar ecological affinities than dry communities (thorny vegetation and *TDDF*); the proportion of grasslands and dry vegetation sums up to 95%. When we associate the pollen percentages of both communities we obtain 75% of dry vegetation in the top-core sample, a percentage that agrees with the high percentages of these biomes in the bio-climate map. Therefore, overall, our semi-quantitative comparison between present-day vegetation in the Godavari basin and the pollen composition of the top-most sample of core NGHP-01-16A (Table 2) indicates that the percentages of the different ecological pollen assemblages follow the proportion of the different biomes in this basin, and therefore no major bias exists between the present-day vegetation and its pollen representation in marine core NGHP-01-16A.

4.2. Vegetation and Indian monsoon variability during the Holocene

The pollen diagram representing the main taxa (i.e. with pollen percentages higher than 5%, is shown in Fig. 3) shows a long-term drying trend on which rapid vegetation shifts are superimposed (Fig. 4). In the early Holocene, from 11,300 years cal BP to 4200 years cal BP, the three humid communities, mangroves, coastal forest and *TMDF* dominated, indicate this time period is the wettest of the entire Holocene. In contrast, from 4200 years cal BP to the present day, climate became more arid as recorded by the increase of both dry vegetation composed of scrub and thorny plants inland and halophyte plants in coastal marshes. Pollen percentage variations of the *TDDF* do not identify, however, a clear change between the early and the end of the Holocene. This biome only needs a moderate water amount to develop, depending on the average humidity. Coastal forest and thorny vegetation expansions likely preclude the development of the *TDDF* during humid and dry periods, respectively. However, the floristic composition of the dry community clearly changed by the progressive replacement of some tropical dry deciduous species with species typical of the thorny vegetation, a drier and more open biome. A distinct climate break is noted at ~4200 years cal BP when the three humid communities in the Godavari basin declined. Overall, these changes show that the Indian monsoon in the CMZ was stronger during the first part of the Early Holocene than during the Late Holocene.

The climatic interpretation of *TDDF* variations changes according to the Holocene period involved, and likely depends on global annual rainfall. During the Holocene humid period, the coastal forest was favored by higher rainfall amount, reducing *TDDF* expansion and representation in the pollen assemblages. In contrast, during the Late Holocene (4200 cal years BP-present *sensu* Walker et al., 2012), when monsoon water availability was reduced, both biomes changed in concert, with common expansions or

Table 2
Comparison between the percentages of different biomes inferred from the pollen assemblages of the top-most core sample of NGHP-16-01 and in those from the Godavari basin bio-climate map (empty box represents lack of data).

Biome	Top core assemblage (%)	Vegetation assemblage (%)
Tropical moist deciduous forest	3	4
Mangrove	1	>1
Coastal forest	0	>1
Marshland	13	>1
Tropical dry deciduous forest	13	21
Thorny vegetation	8	74
Poaceae-Cyperaceae	54	–

contractions indicating relatively strong or weak monsoon conditions. In fact, during the Late Holocene, the rainfall was not strong enough to expand the coastal forest and *TDDF* favoring the thorny vegetation expansion.

Pollen analysis also reveals rapid, millennial to multi-centennial, vegetation variations in terms of biome composition and cover. A series of alternating changes between coastal forest and halophyte biomes indicates that the Holocene in the CMZ (Godavari region) was punctuated by rapid rainfall variations (Fig. 4). Development of a coastal forest due to strong rainfall indicates intense monsoon periods, contrasting with periods of halophyte expansions that correspond to weak monsoon phases. During the wettest period of the Holocene (11,330–4200 years cal BP), two millennial-scale more humid phases are recorded between 5900–7500 years cal BP and 9000–10,400 cal years BP. During the dry period of the Holocene (4200 years cal BP-present), two multi-centennial drier phases occurred around 1600–1200 years cal BP, and 800–300 years cal BP-present, and three wetter phases around 2400–2000 years cal BP, 1200–800 years cal BP and 300 years cal BP to present.

4.3. *Vegetation and Indian monsoon variability during the HS 2 and the last interglacial–glacial transition (MIS 5/4)*

During the time interval corresponding chronologically with the HS 2 (26.2–24.1 kycal BP), almost 70% of the pollen percentage corresponds to grassland plants such as Poaceae and Cyperaceae, the low percentages of halophytes (4%) being explained by a weak marine influence due to the low sea level at that timeat ca. −120 m (Peltier and Fairbanks, 2006). The weak representation of all moist biomes, less than 10%, associated with the high pollen percentages of herbaceous plants and dry community (15%) suggests a dry and open environment (Fig. 5). Clearly, the vegetation records a severe arid period associated with a weak Indian monsoon.

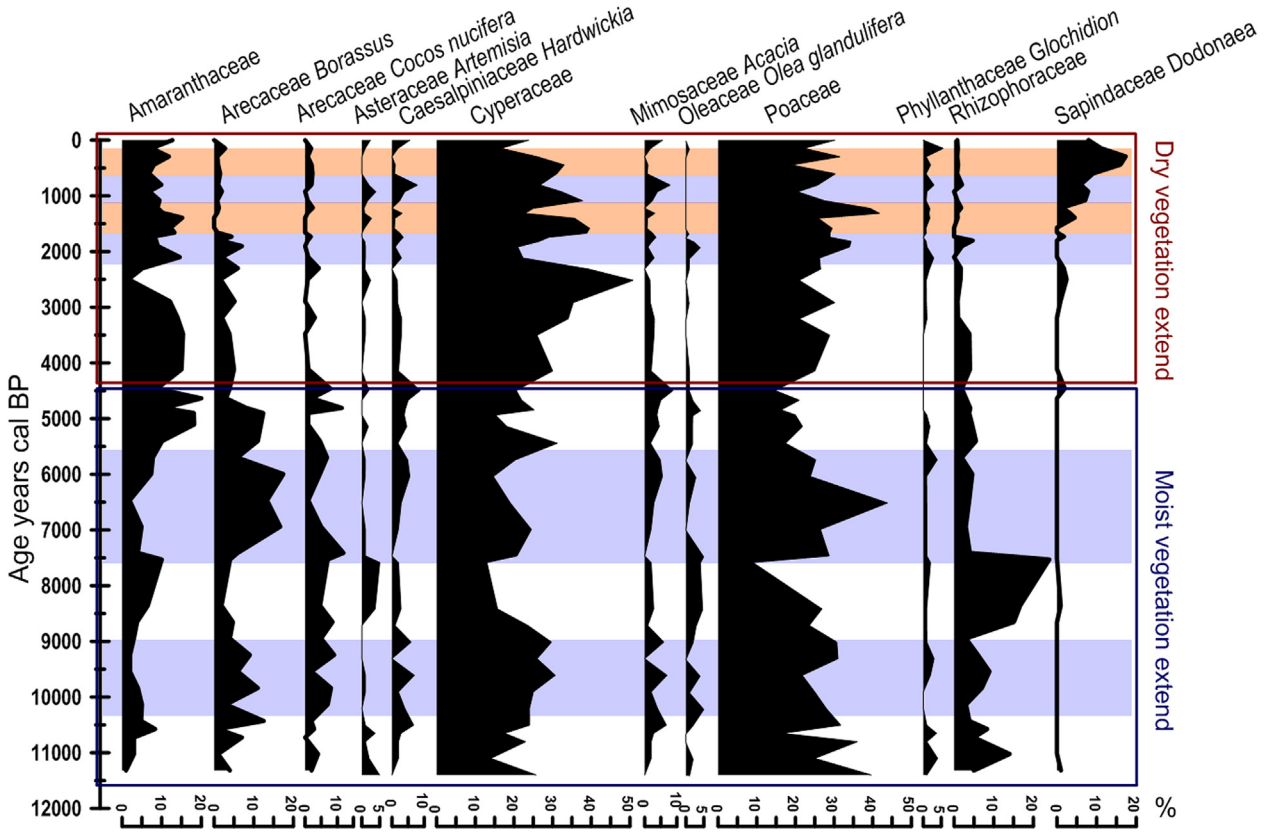

Fig. 3. Pollen diagram with selected morphotypes represented by percentages higher than 5% during the Holocene (core NGHP-01-16A). The detailed pollen diagram is shown in the Supplementary Information.

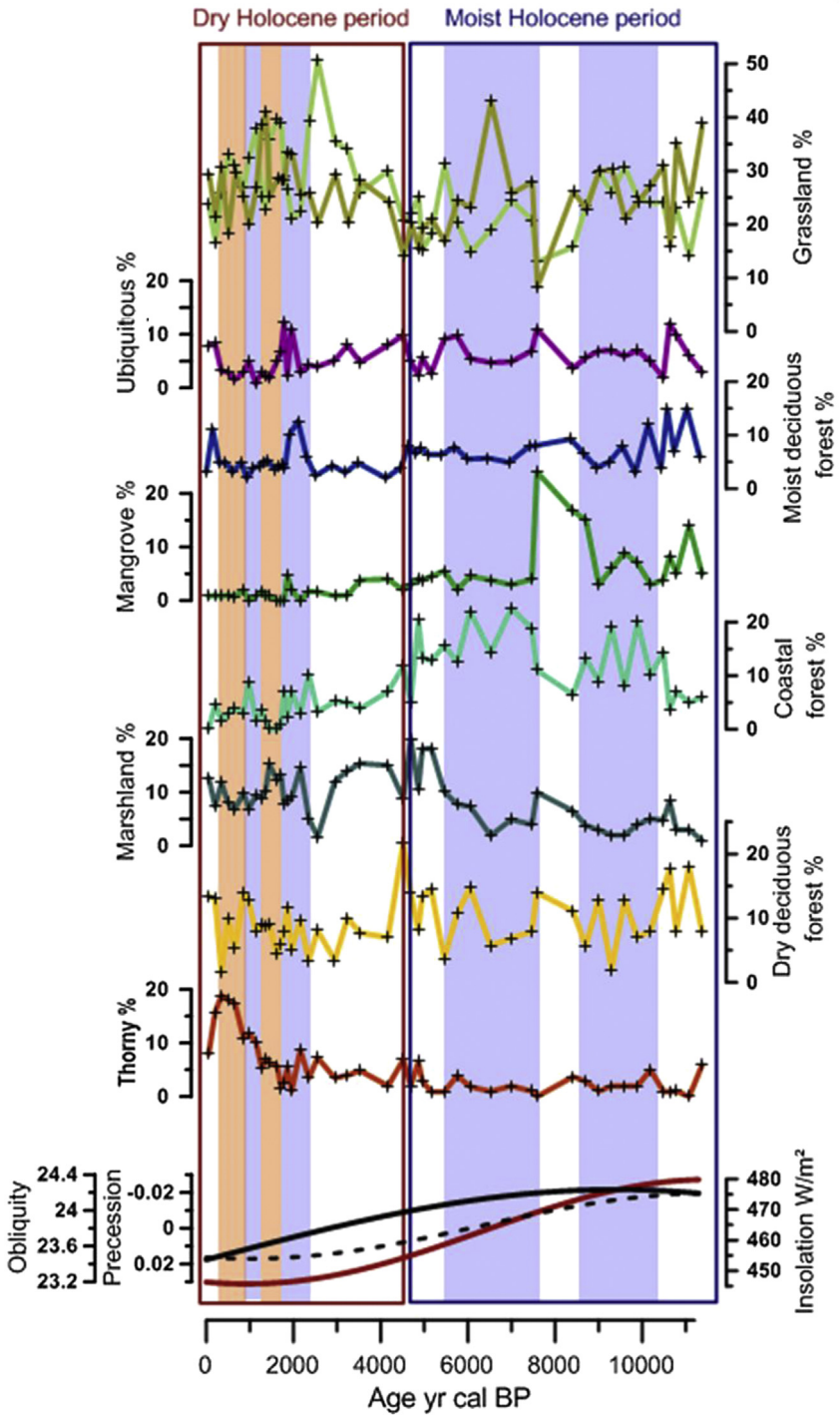

Fig. 4. Variations in the percentages of the different ecological communities along with insolation (red line), precession (dashed line) and obliquity (black line) changes during the Holocene (core NGHP-01-16A). Blue and white bands indicate millennial wet and dry phases, respectively. Orange bands represent historical multi-centennial dry phases (see Figure S3 for statistical significance). Grasslands correspond to Cyperaceaein green and Poaceae in brown. (For interpretation of the references to color in this figure legend, the reader is referred to the web version of this article.)

The MIS 5/4 transition is marked by the high percentages of dry communities, more than 30% (13% halophyte plants, 12% TDDF and 3% Thorny vegetation), and a substantial change in the proportion of the floristic composition of the dry vegetation when compared to that of the previous studied periods: *Artemisia* is particularly well represented with values up to 7% (Fig. 5). During the Holocene and the HS2, *Artemisia* is recorded with average percentages lower than 1% and 2%, respectively. The modern pollen assemblage representing an integrated image of the regional vegetation of the CMZ shows a very low percentage of *Artemisia*. Sutra et al. (1997) show that *Artemisia* was a tracer for dry conditions during the last glacial in Nilgiri hills basin, SW India, covered at present by mountainous evergreen grasslands (Bonnefille et al., 1999; Gupta and Prasad, 1985). In contrast, in the North-Western part of the Indian peninsula, characterized by winter moisture in dry environments weakly affected by the summer monsoon, *Artemisia* is a

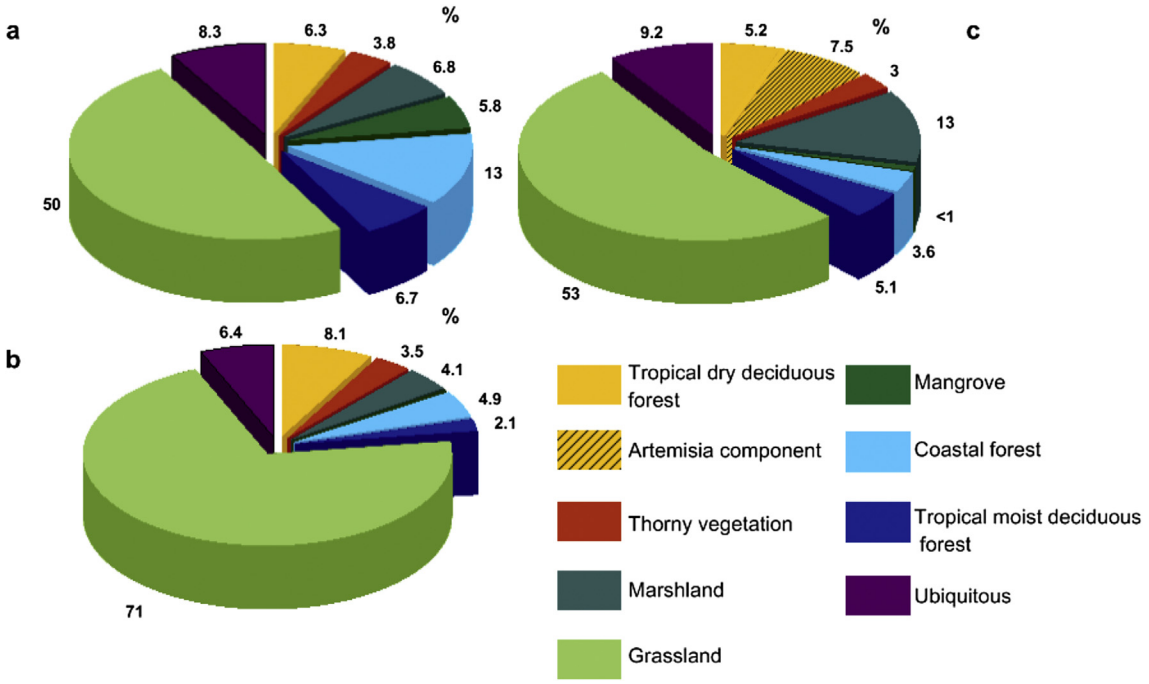

Fig. 5. Comparison of the main ecological communities in Central India during three contrasting climate periods: the moist Holocene phase (core NGHP-01-16A) (a), the Heinrich Stadial 2 (core NGHP-01-16A) (b) and the MIS 5/4 transition (core NHGP-01-19B). The percentage of grasslands includes Cyperaceae and Poaceae.

marker of the influence of both summer and winter Indian monsoons (Demske et al., 2009; Van Campo et al., 1996). In both cases this genus is favored by dry conditions, and considering the relatively low percentage of grasslands during the MIS 5/4 transition (around the same proportion like during the moist Holocene period), *Artemisia* expansion could reflect the increase of winter moisture contrasting with the severe annual dryness observed during the HS 2. Thus, the increase of *Artemisia* during the MIS 5/4 transition may be associated with a weaker seasonality due to the relatively high (low) rainfall amount during the winter (summer) season.

5. Discussion

5.1. Orbital and millennial-scale variability of the Indian monsoon during the Holocene

During the Holocene, the gradual expansion of the main dry taxa (e.g. *Acacia* and/or *Dodonaea*) and halophytic Amaranthaceae followed the reduction of the main moist taxa (e.g. Arecaceae, or *Olea glandulifera*) and of the mangroves (Rhizophoraceae) (Fig. 3). Fig. 4 represents the variation in the proportion of different ecological communities throughout the Holocene. As we mentioned before, the progressive coastal forest decrease records the gradual aridification of the CMZ during the Holocene that was first observed by leaf wax carbon isotope measurements (Ponton et al., 2012), and more recently confirmed by a wide array of palynological and geochemical tracers from the Lonar Lake sequence also located in the CMZ (Prasad et al., 2014). During the Holocene, the moist period between 11,300 and 4200 years cal BP was followed by a period of suppressed Indian summer monsoon. Overall, the monsoon intensity varied in concert with a gradual decrease in insolation. At the beginning of the Holocene, insolation was high, due to maximum obliquity and minimum precession conditions, which increased the contrast between the Indian Ocean and the continent and led to the observed regional intensification of the Indian summer monsoon. After 4200 years cal BP, weak monsoon conditions coincided with low insolation values as the result of decreased obliquity and increased precession forcing (Fig. 4).

During the wet period of the Early Holocene, two wetter phases characterized by maxima in coastal forest development, are well documented at 10,400–9000 cal years BP and 7500–5900 cal years BP. Between these two periods a maximum expansion of mangroves was recorded as a result of an increase in marine influence (Hait and Behling, 2009) with sea level rise documented in the Godavari area between 9000–8000 years BP. The highest percentage of Rhizophoraceae, between 8500 and 7500 years BP, was related to the start of the Godavari delta development between 8400–8000 cal years BP (Rao et al., 2012). According to Blasco et al. (1996), at geological time scales, mangrove expansion is mainly a function of sea level dynamics rather than rainfall variations, even if this ecological community also needs strong fluvial inputs. This seems to be particularly the case of the mangrove increase during the 8400 and 8,000 cal years BP interval when the North Atlantic 8.2 ka cold event should have led to a southward migration of the ITCZ, and consequently a reduction in the Indian monsoon (Dixit et al., 2014).

At present the amount and distribution of *Cocos* and *Borassus*, the main Arecaceae taxa of the coastal forest, are considered as human-controlled (Anupama et al., 2014; Gaussen et al., 1965; Legris, 1963). However, in Central India, sedentary-agriculture is only detected at around 4000 cal years BP as the climate aridified (Asouti and Fuller, 2008; Ponton et al., 2012; Prasad et al., 2014). Therefore, the coastal forest fluctuations that we observe prior to 4000 cal years BP reveal the natural evolution of vegetation, and represent an opportunity to use for the first time, these Arecaceae trees as tracers of the Indian summer monsoon. The strongest humidity period, between 7500–4900 cal years BP, is well correlated with the intense fluvial activity in the Ganga-Brahmaputra mangrove system, located in the North-Eastern part of India, beyond the CMZ boundary (Hait and Belhing, 2009), and with the maximum expansion of the *TMDF* in Lonar Lake (Prasad et al.,

2014). This observation suggest a homogeneous behavior of the Indian summer monsoon in both Godavari and Ganga-Brahmaputra regions during that time interval.

Our record shows a pronounced dry event at 4200 cal years BP, that it is also recorded by the oxygen stable isotope composition of a stalagmite from Mawlmuh Cave, NE India (Berkelhammer et al., 2012). This dry event was a hemispheric-wide worldwide aridification episode that was most pronounced in low- and mid-latitude regions, but is also recorded in various climatic records from high-latitude regions (Walker et al., 2012). This event, which defines the Middle-Late Holocene boundary (Walker et al., 2012), was followed by a progressive monsoon decrease between 4200 and 2500 cal years BP. During the historical period, our high resolution record reveals rapid, multi-centennial, shifts in the Indian monsoon intensity seen in the alternating dominance of two ecologically contrasting biomes: thorny vegetation (dry) and coastal forest (wet) (Fig. 4). A dry episode occurs around 800–300 cal years BP whereas a moist episode is apparent between 1200 and 800 cal years BP. Despite chronological uncertainties, these variations between wet and dry periods could have their counterparts in Europe in the well-characterized Little Ice Age (LIA) and the Medieval Climate Anomaly (MCA) (Desprat et al., 2003). In our pollen assemblage, the dry period, tentatively correlated with the LIA, is well marked by the rise of thorny vegetation and the reduction of the coastal forest, but less well defined by the amount of halophytes. In contrast, the moist period tentatively correlated to the MCA, is characterized by a rise of the coastal forest biome. Previous studies performed on an Arabian Sea sediment core (Agnihotri et al., 2002; Gupta et al., 2003) and on speleothems located in the CMZ (Sinha et al., 2007) show moist and dry phases during MCA and LIA, respectively, and confirm the homogeneous impact of North Atlantic sub-orbital changes on the Indian summer monsoon affecting the entire Indian Peninsula.

Our results show that aridification occurred in the North-Eastern Indian Peninsula contemporaneously with the dry episodes previously identified by Mohtadi et al. (2014) and simulated by models in the Northern Indian Ocean during the Holocene North Atlantic cold spells. To explain the sub-orbital variability of the Indian summer monsoon, models (Broccoli et al., 2006; Chiang and Bits, 2005; Marzin et al., 2012; Vernekar et al., 1995) suggest the operation of feedback mechanisms involving the North Atlantic sea ice cover and fresh water discharges, Himalayan snow cover, and Pacific Ocean temperatures. During the LIA, the strong sea ice expansion in the North Atlantic amplified the cooling in the northern hemisphere and shifted southwards both the polar front and the ITCZ. At the same time, colder SST were recorded in the Pacific Warm Pool (Oppo et al., 2009), that can lead to the decrease of evaporation and relative humidity, and drier winds resulting in a weak monsoon episode. Opposite processes could explain the Indian summer monsoon increase during the MCA, with warm North Atlantic and Pacific SST leading to moister winds in India and a stronger summer monsoon.

During the last 300 years, a decrease in the thorn assemblage and an increase in the *TDDF*, particularly *Hardwickia*, suggest a rise of the Indian summer monsoon, from the end of the dry event identified as the LIA to the present (Fig. 4). The recovery of *Hardwickia* can be however attributed to its cultivation for fodder (Anupama et al., 2014). In contrast to the localized pollen assemblage from Lonar Lake in the Northwestern part of the CMZ (Prasad et al., 2014), there are no direct markers of human activities in our record, except *Xanthium*, which is recorded sporadically and in low proportions only in the top part of the core. This observation attests that the climatic signal is well delineated in our marine pollen record and that it represents an integrated image of the regional vegetationeven if human activities locally affected the Godavari basin since 4000 BP (Ponton et al., 2012).

5.2. Indian monsoon variations under three different climate boundary conditions (Holocene, HS 2 and MIS 5/4)

We compared the mean state of the CMZ vegetation during the wettest period of the Holocene, maximum in boreal summer insolation, to the last glacial coldest events in the North Atlantic (HS 2), and the last interglacial–glacial transition (MIS 5/4) (Fig. 5). The number of samples used to reconstruct the pollen assemblages varies between the three studied time intervals (i.e., 25 for the Holocene, 2 for the HS2 and 13 for the MIS 5/4 transition); therefore a methodological bias cannot be eliminated. Nevertheless, we do not quantify differences, but instead qualitatively discuss the main characteristics of Indian summer monsoon behavior during the three distinct climate contexts as expressed by pollen in CMZ. Our results reveal substantial contrasts: the first part of the Holocene is the most humid period (highest seasonality: maximum in summer monsoon associated with winter monsoon minima), the HS 2 is the driest, and the MIS 5/4 transition is characterized by a low seasonal contrast (relatively moist winters and dry summers). The contrast between a drier HS 2 event and wetter Holocene is consistent with observations of increased C4 plant material, increased heavy/magnetic mineral content (reduced weathering), and enhanced productivity (reduced stratification) between 70 and 10 ka recently documented at NGHP-01-19B (Phillips et al., 2014b).

During the HS 2, the low boreal summer insolation (high precession and low obliquity) associated with a cold and fresh event in the North Atlantic can explain the drastic reduction of Indian summer monsoon (Marzin et al., 2012). Southward shifts of the ITCZ are recorded in the Indian Ocean during other Heinrich events (Gibbons et al., 2014) and can explain the strong aridity during the HS 2. Modeling experiments by Pausata et al. (2011) suggest that the sea ice expansion in the North Atlantic generates a cooling in the high-mid latitudes of the Northern Hemisphere, and colder and drier air in the North of the Indian Ocean. Low temperature contrast between the land and the sea, drier winds, and southward ITCZ position may explain the strong reduction of moisture recorded by the vegetation in Central India.

During the MIS 5/4 boundary interval (70,000–80,000 years cal BP), open and dry vegetation indicates a low monsoon intensity. Gupta et al. (2003) show the same trend during the MIS 7/6 transition. The orbital parameters account for a weak monsoon period due to a lower insolation in comparison with the Holocene wet period (i.e., obliquity is lower and precession is higher (Marzin and Braconnot, 2009)). Feedback mechanisms such as ice sheet growth, the expansion of Tibetan Plateau snow cover or the reduction of moisture from the Indian Ocean could reinforce the decrease in insolation. A new ecological assemblage composed of *Artemisia* reveals a low seasonality during the MIS 5/4 transition induced by low obliquity and high precession. This ice growth period is marked in the Indian peninsula by a reduction of the summer monsoon, but weaker than that during the HS 2, and/or a rise of winter monsoon.

The particular dry conditions during the HS 2 could result from a combination of two factors: a particularly low seasonal contrast due to high precession and especially large iceberg discharges in the North Atlantic Ocean. Contrary to strong Heinrich events such as HS 2, Sanchez Goñi et al. (2013) show weak freshwater discharges during the MIS 5/4 transition, and persistence of a warm surface current in the Eastern North Atlantic bringing humidity to the northern high latitudes. Via atmospheric teleconnections, the strongest iceberg discharges in the North Atlantic Ocean contribute

to a more southern position of the ITCZ in the Indian peninsula during HS 2 than during the MIS 5/4 transition, both occurring under a context of low seasonality; this rapid feedback mechanism could explain the weaker monsoon rainfall and the severe drought in Central India during the HS 2. Gibbons et al. (2014) and Donohoe et al. (2013) propose a strong relationship between inter-hemispheric temperature gradient and the ITCZ position in both modern and past records. Their hypothesis envisionsan atmospheric teleconnection between tropical areas and the North Atlantic Ocean driven by Rossby wave-trains and leading to a reorganization of Hadley circulation (southern position of an ITCZ branch) during the cold spells in the North Atlantic Ocean (Mohtadi et al., 2014). If the ENSO-controlled Indian Ocean SST variations seem to affect theamount of moisture that the westerlies bring to the Indian monsoon system (Clement et al., 1999; Gibbson et al., 2014), our data suggest, in line with Prasad et al. (2014), that Indian summer rainfall distribution is preferentially impacted by the ITCZ position (in link with insolation feedback mechanisms) than by ENSO at centennial, millennial and glacial/interglacial scales.

6. Conclusions

The similarity between the pollen-inferred vegetation of the top-most sample of core NGHP-01-16A and the present-day proportion of the different biomes in the Godavari basin, as shown by the Indian bio-climate map, emphasizes the relevance of using pollen grains preserved in marine cores to reconstruct past regional vegetation and climate variations. Vegetation records of Godavari and Mahanadi basins, both located in the CMZ, reflect the changes in rainfall distribution and monsoon intensity in Central India during three contrasting climatic periods. Variability in pollen from cores NGHP-01-16A and NGHP-O1-19B-2H1 shows changes in the relative dominance of three distinct vegetation types: the Early-Middle Holocene (11,700 years cal BP-4200 years cal BP) is marked by the expansion of a coastal forest due to an increase in wet conditions, the HS 2 period is characterized by dry vegetation and climate, and the last start of a glaciation (MIS 5/4 transition) by an increase (decrease) of winter (summer) monsoon. Our vegetation record identifies an alternation of moist and dry events in Central India during the historical period that may correlate with the MCA and LIA, respectively. The monsoonal-driven aridification trend observed for the Holocene, and the weak (strong) summer(winter) monsoon, recognized for the first time by our study of the MIS 5/4 transition, shows that insolation variations substantially impact Indian monsoon intensity and seasonality, i.e. the average monsoon rainfall rises (decreases) with a strong (weak)land-sea contrast due to a strong (weak) summer insolation. Both HS 2 and MIS 5/4 periods were characterized by low boreal summer insolation, but the vegetation in Central India and, therefore the regional climate, were different. The severe drought recorded during HS 2 was probably the result of large iceberg discharges in the North Atlantic Ocean, which by feedback processes affected ITCZ position and summer monsoon intensity in CMZ of India. In contrast, moderate iceberg discharges led to a less dry climate during the start of the last glaciation at the MIS 5/4 transition. In agreement with model predictions (Pausata et al., 2011; Gibbson et al., 2014), our study suggests that feedback mechanisms are determinant processes to explain the magnitude and distribution of monsoon rainfalls, especially at millennial times scales. Freshwater inputs in the North Atlantic Ocean, the ITCZ location and the Indian Ocean surface temperatures are some feedbacks that change the hydrological cycle in tropical areas and control rainfall distribution and intensity in Central India over geological time scales.

Acknowledgments

The work of C.Z. was supported by the ANR MONOPOL. We thank NGHP-01 Expedition personnel for core collection and post-cruise access. Many thanks to S. Desprat for hierchical clustering analysis on the Holocene samples and M.H. Castera and O. Ther for invaluable technical assistance. We also thank the UMR EPOC and the French Institute of Pondicherry for their welcome. The authors are grateful to the editor and the anonymous referee for their helpful comments.

Appendix A. Supplementary data

Supplementary data related to this article can be found at http://dx.doi.org/10.1016/j.quascirev.2015.06.009.

References

Agnihotri, R., Dutta, K., Bhushan, R., Somayajulu, B.L.K., 2002. Evidence for solar forcing on the Indian monsoon during the last millennium. Earth Planet. Sci. Lett. 198, 521–527.
Anupama, K., Prasad, S., Reddy, S.C., 2014. Vegetation, land cover and land use changes of the last 200 years in the Eastern Ghats (southern India) inferred from pollen analysis of sediments from a rain-fed tank and remote sensing. Quat. Int. 325, 93–104.
Araya-Melo, P.A., Crucifix, M., Bounceur, N., 2014. Global sensitivity analysis of Indian Monsoon during the Pleistocene. Clim. Past Discuss. 10 (2), 1609–1651.
Asouti, E.D., Fuller, Q., 2008. Trees and Woodlands in South India. In: Archaeological Perspectives. Left Coast, Walnut Creek, Calif.
Attri, S.D., Tyagi, A., 2010. Climate profile of India. Contrib. Indian Netw. Clim. Change Assess. Natl. Commun.-Ii Minist. Environ. For. 1501, 1–129.
Blasco, F., Saenger, P., Janodet, E., 1996. Mangroves as indicators of coastal change. Catena 27, 167–178.
Bonnefille, R., Anupama, K., Barboni, D., Pascal, J., Prasad, S., Sutra, J.P., 1999. Modern pollen spectra from tropical South India and Sri Lanka: altitudinal distribution. J. Biogeogr. 26, 1255–1280.
Broccoli, A.J., Dahl, K.A., Stouffer, R.J., 2006. Response of the ITCZ to Northern Hemisphere cooling. Geophys. Res. Lett. 33 (1), L01702.
Berkelhammer, M., Sinha, A., Stott, L., Cheng, H., Pausata, F.S.R., Yoshimura, K., 2012. An abrupt shift in the Indian monsoon 4000 years ago. Clim. Landsc. Civiliz. 75–88.
Caley, T., 2011. De l'importance de l'Océan indien pour les paleoclimats quaternaires: la mousson et le courant des aiguilles. Université de Bordeaux.
Chiang, J.C., Bitz, C.M., 2005. Influence of high latitude ice cover on the marine Intertropical Convergence Zone. Clim. Dyn. 25, 477–496.
Clement, A.C., Seager, R., Cane, M.A., 1999. Orbital controls on the El Niño Southern Oscillation and the tropical climate. Paleoceanography 14 (4), 441–456.
Collett, T.S., Riedel, M., Cochran, J.R., Boswell, R., Kumar, P., Sathe, A.V., 2008. Indian Continental Margin Gas Hydrate Prospects: Results of the Indian National Gas Hydrate Program (NGHP) Expedition 01.
Demske, D., Tarasov, P.E., Wünnemann, B., Riedel, F., 2009. Late glacial and Holocene vegetation, Indian monsoon and westerly circulation in the Trans-Himalaya recorded in the lacustrine pollen sequence from TsoKar, Ladakh, NW India. Palaeogeogr. Palaeoclimatol. Palaeoecol. 279 (3), 172–185.
Desprat, S., Sánchez Goñi, M.F., Loutre, M.F., 2003. Revealing climatic variability of the last three millennia in northwestern Iberia using pollen influx data. Earth Planet. Sci. Lett. 213 (1), 63–78.
Dixit, Y., Hodell, D.A., Sinha, R., Petrie, C.A., 2014. Abrupt weakening of the Indian summer monsoon at 8.2 kyr BP. Earth Planet. Sci. Lett. 391 (1), 16–23.
Donohoe, A., Marshall, J., Ferreira, D., McGee, D., 2013. The relationship between ITCZ location and cross equatorial atmospheric heat transport from the seasonal cycle to the Last Glacial Maximum. Int. J. Clim. 26, 3597–3618.
Dupont, L.M., Wyputta, U., 2003. Reconstructing pathways of aeolian pollen transport to the marine sediments along the coastline of SW Africa. Quat. Sci. Rev. 22 (2), 157–174.
Dutta, K., Bhushan, R., Somayajulu, B.L., 2001. Delta R correction values for the northern Indian Ocean. Radiocarbon 43, 483–488.
Fleitmann, D., Burns, S.J., Mangini, A., Mudelsee, M., Kramers, J., Villa, I., Neff, U., Al-Subbary, A.A., Buettner, A., Hippler, D., Matter, A., 2007. Holocene ITCZ and Indian monsoon dynamics recorded in stalagmites from Oman and Yemen (Socotra). Quat. Sci. Rev. 26 (1), 170–188.
Gadgil, S., 2003. The Indian monsoon and its variability. Annu. Rev. Earth Planet. Sci. 31 (1), 429–467.
Gaussen, H., Legris, P., Viart, M., Meher-Homji, V.M., 1965. Godavari and Mahanadi Maps and Booklets. IFP.
Gaussen, H., Legris, P., Viart, M., Meher-Homji, V.M., 1963–1973. Maps-ifp.
Gibbons, F.T., Oppo, D.W., Mohtadi, M., Rosenthal, Y., Cheng, J., Liu, Z., Linsley, B.K., 2014. Deglacial δ18O and hydrologic variability in the tropical Pacific and Indian Oceans. Earth Planet. Sci. Lett. 387, 240–251.

Gunnell, Y., 1997. Relief and climate in South Asia: the influence of the Western Ghats on the current climate pattern of Peninsular India. Int. J. Clim. 17, 1169–1182.
Gupta, A.K., Anderson, D.M., Overpeck, J.T., 2003. Abrupt changes in the Asian southwest monsoon during the Holocene and their links to the North Atlantic Ocean. Nature 421, 354–357.
Gupta, H.P., Prasad, K., 1985. The vegetation development during 30 000 years BP at Colgrain, Ootacamund, Nilgiris, S. India. J. Palynol. 21, 174–187.
Hahn, D.G., Shukla, J., 1976. An apparent relationship between Eurasian snow cover and Indian monsoon rainfall. J. Atmos. Sci. 33 (12), 2461–2462.
Hait, A.K., Behling, H., 2009. Holocene mangrove and coastal environmental changes in the western Ganga–Brahmaputra Delta, India. Veg. Hist. Archaeobotany 18 (2), 159–169.
Heusser, C.J., 1985. Quaternary Pollen Records from the Pacific Northwest Coast: Aleutians to the Oregon-California Boundary. AASP Foundation, p. 25.
Imbrie, J., Hays, J.D., Martinson, D.G., McIntyre, Mix, A.C., Morely, J.J., Pisias, N.G., Prell, W.L., Shackleton, N.J., 1984. The orbital theory of Pleistocene climate: support from a revised chronology of the marine δ18O record. In: Berger, A.L., et al. (Eds.), Milankovitch and Climate, 1, pp. 269–305.
Johnson, D., 2010. Tropical palms: 2010 revision. Non-wood For. Prod. 10 (1), 9–171.
Johnson, J.E., Phillips, S.C., Torres, M.E., Piñero, E., Rose, K.K., Giosan, L., 2014. Influence of total organic carbon deposition on the inventory of gas hydrate in the Indian continental margins. Mar. Pet. Geol. 58, 406–424. http://dx.doi.org/10.1016/j.marpetgeo.2014.08.021.
Juggins, S., 2009. Package "rioja" – Analysis of Quaternary Science Data. The Comprehensive R Archive Network.
Kraus, M., Matthiessen, J., Stein, R., 2003. A Holocene marine pollen record from the northern Yenisei Estuary, southeastern Kara Sea, Siberia. Mar. Sci. 6, 435–456.
Legris, P., 1963. La végétation de l'Inde. Ecologie et flore. In: Travaux de la Section Scientifique et Technique 6. Institut Français de Pondicherry.
Martinson, D.G., Pisias, N.G., Hays, J.D., Imbrie, J., Moore, T.C., Shackleton, N.J., 1987. Age dating and the orbital theory of the ice ages: development of a high resolution 0 to 300,000 year chronostratigraphy. Quat. Res. 27, 1–29.
Marzin, C., Braconnot, P., 2009. Variations of Indian and African monsoons induced by insolation changes at 6 and 9.5 kyr BP. Clim. Dyn. 33 (2–3), 215–231.
Marzin, C., Kallel, N., Kageyama, M., Duplessy, J.C., Braconnot, P., 2012. Glacial fluctuations of the Indian monsoon and their relationship with North Atlantic abrupt climate change: new data and climate experiments. Clim. Past Discuss. 8 (6), 6269–6308.
Mohtadi, M., Prange, M., Oppo, D.W., De Pol-Holz, R., Merkel, U., Zhang, X., Steinke, S., Lückge, A., 2014. North Atlantic forcing of tropical Indian Ocean climate. Nature 509, 76–80.
Naughton, F., Sanchez Goñi, M.F., Desprat, S., Turon, J.L., Duprat, J., Malaizé, B., Joli, C., Cortijo, E., Drago, T., Freitas, M.C., 2007. Present-day and past (last 25000 years) marine pollen signal off western Iberia. Mar. Micropaleontol. 62 (2), 91–114.
Oppo, D.W., Rosenthal, Y., Linsley, B.K., 2009. 2,000 years long temperature and hydrology reconstructions from the Indo-Pacific warm pool. Nature 460, 1113–1116.
Pausata, F.S., Battisti, D.S., Nisancioglu, K.H., Bitz, C.M., 2011. Chinese stalagmite δ18O controlled by changes in the Indian monsoon during a simulated Heinrich event. Nat. Geosci. 4, 474–480.
Peltier, W.R., Fairbanks, R.G., 2006. Global glacial ice volume and Last Glacial Maximum duration from an extended Barbados sea level record. Quat. Sci. Rev. 25 (23), 3322–3337.
Phillips, S.C., Johnson, J.E., Underwood, M.B., Guo, J., Giosan, L., Rose, K., 2014a. Long-timescale variation in bulk and clay mineral composition of Indian continental margin sediments in the Bay of Bengal, Arabian Sea, and Andaman Sea. Mar. Pet. Geol. 58, 117–138. http://dx.doi.org/10.1016/j.marpetgeo.2014.06.018.
Phillips, S.C., Johnson, J.E., Giosan, L., Rose, K., 2014b. Monsoon-influenced variation in productivity and lithogenic sediment flux since 110 ka in the offshore Mahanadi Basin, northern Bay of Bengal. Mar. Pet. Geol. 58, 502–525. http://dx.doi.org/10.1016/j.marpetgeo.2014.05.007.
Ponton, C., Giosan, L., Eglinton, T.I., Fuller, D.Q., Johnson, J.E., Kumar, P., Collett, T.S., 2012. Holocene aridification of India. Geophys. Res. Lett. 39, L03704.
Prasad, S., Anoop, A., Riedel, N., Sarkar, S., Menzel, P., Basavaiah, N., Krishnan, R., Fuller, D., Plessen, B., Gaye, B., Rohl, U., Wilkes, H., Sachse, D., Sawant, R., Wiesner, M.G., Stebich, M., 2014. Prolonged monsoon droughts and links to Indo-Pacific warm pool: a Holocene record from Lonar Lake, central India. Earth Planet. Sci. Lett. 391, 171–182.
Pullaiah, T., Chennaiah, E., Ali Moulali, D., Karappusamy, S., 1997. Flora of Andhra Pradesh (India). Scientific publishers, jodhur.
Rao, K.N., Saito, Y., Nagakumar, K.C.V., Demudu, G., Basavaiah, N., Rajawat, A.S., Tokanai, F., Kato, K., Nakashima, R., 2012. Holocene environmental changes of the Godavari Delta, east coast of India, inferred from sediment core analyses and AMS ^{14}C dating. Geomorphology 175, 163–175.
Raveejan, M., Gadgil, S., 2008. Active and Break Speels of the Indian Summer Monsoon. NNC Reseacher report.
Reimer, P.J., et al., 2009. IntCal09 and Marine09 radiocarbon age calibration curves, 0-50,000 years cal BP. Radiocarbon 51 (4), 1111–1150.
Ruddiman, W.F., Kutzbach, J.E., 1991. Plateau uplift and climatic change. Sci. Am. 264, 66–72.
Sánchez Goñi, M.F., Bard, E., Landais, A., Rossignol, L., d'Errico, F., 2013. Air-sea temperature decoupling in western Europe during the last interglacial-glacial transition. Nat. Geosci. 6 (10), 837–841.
Selvam, V., 2003. Environmental classification of mangrove wetlands of India. Curr. Sci. 84 (6), 757–765.
Sinha, A., Cannariato, K.G., Stott, L.D., Cheng, H., Edwards, R.L., Yadava, M.G., Ramesh, R., Singh, I.B., 2007. A 900-year (600 to 1500 AD) record of the Indian summer monsoon precipitation from the core monsoon zone of India. Geophys. Res. Lett. 34, L16707.
Southon, J., Kashgarian, M., Fontugne, M., Metivier, B., Yim, W.W.S., 2002. Marine reservoir corrections for the Indian Ocean and southeast Asia. Radiocarbon 44 (1), 167–180.
Stuiver, M., Reimer, P.J., 1993. Extended C-14 data-base and revised calib 3.0 C-14 age calibration program. Radiocarbon 35 (1), 215–230.
Sutra, J.P., Bonnefille, R., Fontugne, M., 1997. Etude palynologique d'un nouveau sondage dans les marais de Sandynallah (massif des Nilgiri, Sud-Ouest de l'Inde). Géogr. Phys. Quat. 51 (3), 415–426.
Van Campo, E., Cour, P., Sixuan, H., 1996. Holocene environmental changes in Bangong Co basin (Western Tibet). Part 2: the pollen record. Palaeogeogr. Palaeoclimatol. Palaeoecol. 120 (1), 49–63.
Vernekar, A.D., Zhou, J., Shukla, J., 1995. The effect of Eurasian snow cover on the Indian monsoon. J. Clim. 8 (2), 248–266.
Walker, M.J.C., Berkelhammer, M., Björck, S., Cwynar, L.C., Fisher, D.A., Long, A.J., Lowe, J.J., Newnham, R.M., Rasmussen, S.O., Weiss, H., 2012. Formal subdivision of the Holocene Series/Epoch: a Discussion Paper by a Working Group of INTIMATE (Integration of ice-core, marine and terrestrial records) and the Subcommission on Quaternary Stratigraphy (International Commission on Stratigraphy). Quat. Sci. 27 (7), 649–659.
Walter, H., 1961. Etude de l'influence du climat et plus particulièrement des périodes de sécheresses entre les moussons sur la végétation humide de l'Inde. Rapport UNESCO.
Webster, P.J., Magafia, V.O., Palmer, T.N., Shukla, J., Tomas, R.A., Yanai, M., Yasunari, T., 1998. Monsoons: processes, predictability, and the prospects for prediction. J. Geophys. Res. 103, 14,451–14,510.
Yihui, D., Chongyin, L., Yanju, L., 2004. Overview of the South China Sea monsoon experiment. Adv. Atmos. Sci. 21 (3), 343–360.